3

Chapter 3

Mixed Convective Slip Flow and Heat Transport for Visco-Elastic Fluid Past a Vertical Plate

3.1 Introduction

The heat transition due to the combined effects of pressure and buoyancy forces for boundary layer past a plate is extensively studied these days because of its wide applications in manufacturing processes. The application of such flow is often observed in solar and electronic devices, nuclear reactors, heat exchangers, lubrication, and drying processes. The mixed convective flow which arises due to the interaction of pressure and buoyant forces influences the amount of heat transfer. Mukhopadhyay *et al.* [55] demonstrated the magnetohydrodynamic heat flow due to mixed convection past a vertical porous surface with slip effects. Das *et al.* [56] presented the MHD mixed convective fluid flow in an inclined permeable plate taking viscous dissipation and Joule heating into consideration. Aurangzaib *et al.* [57] examined the mixed convective unsteady stagnation point slip flow on a shrinking sheet. The study revealed that the surface velocity enhances due to slip at the sheet. Prasannakumara *et al.* [58] investigated the impact of thermal radiation along with slip flow and heat transfer of fluid containing nanoparticles over a

permeable stretching sheet. Ellahi *et al.* [59] examined the hydromagnetic entropy generation and slip effect on heat transport for the boundary layer flow past a moving flat plate. The effect of Hall and ion-slip on mixed convective flow for nanofluid past a permeable stretching sheet is investigated by Ibrahim *et al.* [60]. Dey and Nath [61] presented the mixed convective steady fluid flow over a vertical plate without viscous dissipation whereas the theoretical investigation of mixed convective viscous incompressible boundary layer external fluid flow past a moving vertical plate taking viscous dissipation into account was carried out by Bachok *et al.* [62].

The fluid-particle when comes in contact with a solid boundary often slips without taking the velocity of the surface due to its own fixed tangential velocity. This type of flow is called slip flow and such flow is often observed in polymer and adhesive solutions. The fluids which exhibit slip flow have many practical applications in the chemical polishing industry. Bhattacharyya *et al.* [50] investigated the effects of slip parameter for Newtonian boundary layer fluid flow over a moving flat plate and found that the fluid motion is significantly affected under the influence of slip parameter. Cao *et al.* [51] presented the effects of slip on laminar mixed convection and heat transfer over a vertical plate. The numerical solution carried out in this study to observe flow parameters impact on the velocity and temperature distribution. Aziz [63] examined the hydromagnetic boundary layer fluid flow past a flat plate taking slip flow and heat flux surface condition. The study explored the constant heat flux boundary conditions. Patil *et al.* [48] presented the parallel stream mixed convection fluid flow for unsteady case taking a vertical moving plate.

The non-Newtonian visco-elastic fluid pertaining viscous and elastic nature has lots of practical applications in different fields of engineering sciences. When pressure is applied to it with the high velocity it hardens and changes its state from liquid to solid. That's why these days it is widely used in protective equipment like liquid body armor, liquid sports shoes, helmet, mobile case, speed bump, etc. Hayat *et al.* [64] demonstrated the heat transport for mixed convection taking visco-elastic fluid through a stretching cylinder. The hydromagnetic mixed convective visco-elastic fluid motion and transition of heat past a permeable wedge in presence of thermal radiation was investigated by Rashidi *et al.* [36].

The above literature survey shows that very little work has been carried out to heat transport problems considering the non-Newtonian visco-elastic fluid model in the slip flow regime and thus the present paper aims to investigate the heat transition due to mixed

convection for boundary layer visco-elastic fluid over a vertical plate with slip condition. The visco-elasticity of the fluid exhibits by the non-Newtonian fluid model Walters Liquid (Model $B^{'}$). The resultant equations guiding fluid motion are obtained by using similarity variables. The MATLAB inbuilt solver 'bvp4c' is applied for computation. The evaluated results are plotted for discussions to observe the effects of involved dominant flow parameters.

3.2 Mathematical Formulation

The motion of steady mixed convective incompressible visco-elastic boundary layer fluid past a vertical plate with slip condition factor is considered. Fig. 3.1 depicts the geometry of fluid motion. The fluid flow governed by equations of continuity, motion and energy is written taking boundary layer approximations as:

$$u_x + v_y = 0 \tag{3.2.1}$$

$$uu_x + vu_y = \nu u_{yy} - \frac{k_0}{\rho}\left(uu_{xyy} + vu_{yyy} - u_y u_{xy} - v_y u_{yy}\right) + g\,\beta^*(T - T_\infty) \tag{3.2.2}$$

$$uT_x + vT_y = \left(\frac{K}{\rho C_p}\right) T_{yy} \tag{3.2.3}$$

The lower subscripts of u, v, and T in terms of x and y denote the derivatives of respective order and other symbols have their usual meaning as stated above.

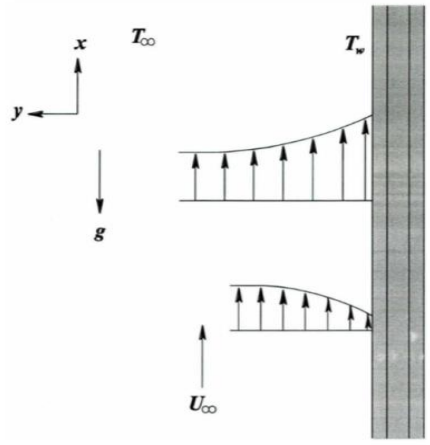

Fig. 3.1 The geometrical flow model

The conditions imposed at the boundary are:

$$u = L_1 u_y\,, v = 0 \text{ at } y = 0; \quad u \to U_\infty \text{ as } y \to \infty \tag{3.2.4}$$

$T = T_W + D_1 T_y$ at y = 0 ; $T \to T_\infty$ as $y \to \infty$ (3.2.5)

where, $L_1 = L_0 (Re_x)^{\frac{1}{2}}$: velocity slip factor,

$D_1 = D_0 (Re_x)^{\frac{1}{2}}$: thermal slip factor,

$Re_x = \frac{U_\infty x}{\nu}$: Reynolds number,

L_0 and D_0: initial values of slip factors,

$T_W = T_\infty + \frac{T_0}{x}$: variable plate temperature with T_0constant,

U_∞: free stream velocity.

Similarity transformations have taken after careful investigation as

$$\Psi = \sqrt{U_\infty \nu x}\, f(\xi), \qquad T = T_\infty + (T_w - T_\infty)\theta(\xi) \quad and \quad \xi = \frac{y}{x}\sqrt{Re_x} \tag{3.2.6}$$

where Ψ and ξ represent stream function and similarity variable respectively with

$u = \frac{\partial \Psi}{\partial y}$ and $v = -\frac{\partial \Psi}{\partial x}$.

Applying similarity transformations (3.2.6), equations (3.2.2) and (3.2.3) finally reduced to the forms:

$$f''' + \frac{1}{2} f f'' + k_1 [2 f' f''' + f f'^{\mathrm{v}} - (f'')^2] + \lambda\theta = 0 \tag{3.2.7}$$

$$\theta'' + Pr\left(\frac{1}{2} f\theta' + f'\theta\right) = 0 \tag{3.2.8}$$

where dashes denote differentiation with respect to ξ and

$k_1 = \frac{k_0 U_\infty}{2\mu x}$: modified visco-elastic parameter,

$\lambda = \frac{g\beta^* T_0}{U_\infty^2}$: mixed convection parameter,

$Pr = \frac{\mu C_p}{K}$: Prandtl number.

The final reduced form of conditions (3.2.4) and (3.2.5) at the boundary are

$$f(\xi) = 0,\ f'(\xi) = \delta f''(\xi)\ at\ \xi = 0\ ; \qquad f'(\xi) \to 1,\ f''(\xi) \to 0\ as\ \xi \to \infty \tag{3.2.9}$$

$$\theta(\xi) = 1 + \beta\theta'(\xi) at\ \xi = 0\ ;\ \theta(\xi) \to 0\ as\ \xi\ \to \infty \tag{3.2.10}$$

3.3 Method of Solution

The Matlab solver 'bvp4c' is a collocation method employed to solve a system of linear or non-linear BVP. This method is different from the shooting method and it is based on an algorithm. It can compute inexpensively the approximate value of $y(x)$ for any x in $[a, b]$ taking boundary conditions at every step. In this method, the boundary conditions at infinity are replaced with one at a finite point which reasonably satisfies the given problem. To apply finite difference method-based solver 'bvp4c', the resultant governing equations (3.2.7) and (3.2.8) are transformed as follows:

$$f = g_1, f' = g_2,\ f'' = g_3, f''' = g_4\ , \theta = g_5, \theta' = g_6 \tag{3.3.1}$$

From (3.3.1), we can write

$$g_1' = g_2, g_2' = g_3, g_3' = g_4, g_5' = g_6 \tag{3.3.2}$$

Using (3.3.1) and (3.3.2), equations (3.2.7) and (3.2.8) can be written as:

$$g_4' = \frac{1}{g_1}\left[(g_3)^2 - 2g_2g_4 - \left(\frac{1}{k_1}\right)\left(g_4 + \frac{1}{2}g_1g_3 + \lambda g_5\right)\right] \tag{3.3.3}$$

$$g_6' = -Pr\left(\frac{1}{2}g_1g_6 + g_2g_5\right) \tag{3.3.4}$$

and the boundary conditions (3.2.9) and (3.2.10) takes the following forms:

$$g_1(0) = 0, g_2(0) = \delta g_3(0)\ and\ \ g_2(\infty) = 1, g_3(\infty) = 0 \tag{3.3.5}$$

$$g_5(0) = 1 + \beta g_6(0)\ and\ \ g_5(\infty) = 0 \tag{3.3.6}$$

The numerical computation is carried out by the solver 'bvp4c' with the help of the above transformed results.

3.4 Results and Discussions

To investigate the effects of flow feature parameters on the velocity profile $f'(\xi)$, temperature profile $\theta(\xi)$, temperature gradient profile $\theta'(\xi)$ and temperature gradient at the plate $-\theta'(0)$numerical evaluation is carried out with the help of 'bvp4c' MATLAB

solver. The computed results are represented graphically for discussion to bring out clear physical insight into the flow problem.

To validate the numerical method employed in the present work and to judge the accuracy of the obtained results, a comparison is carried out for $f''(0)$ and $-\theta'(0)$with the published results of Dey and Nath (1981), and Bachok et al. (2013) with two different values of λ and other involved flow parameters. The obtained results of the present study are found in excellent accord with the earlier published results, as shown in Table 1.

Table 3.1. Comparison of $f''(0)$ and $-\theta'(0)$ for two different values of λ with $k_1 =$ $\delta = \beta = 0$ with $Pr = 1$.

	Dey and Nath (1981)		Bachok et al. (2013)		Present Work	
λ	$f''(0)$	$-\theta'(0)$	$f''(0)$	$-\theta'(0)$	$f''(0)$	$-\theta'(0)$
-0.1	0.350971	0.760608	0.350986	0.760823	0.3507	0.7608
0.1	0.332920	0.593633	0.332920	0.593633	0.3329	0.5936

Fig. 3.2 to 3.5 are plotted to illustrate the effects of k_1, λ, δ, and β on the velocity profile. The velocity profile $f'(\xi)$ approaches to 1 very rapidly as $\xi \rightarrow 5$ and thus taking 5 as infinity appears to be justify the boundary conditions at infinity. The fluid motion accelerated with increasing values of visco-elasticity as seen from Fig. 3.2. The slip condition at the boundary allows a large amount of fluid slips along with the plate which in turn accelerates the fluid motion. Fig. 3.3 indicates that the rate of fluid flow increases with the rise of mixed convection controlling parameter as it gives suitable buoyancy impact with slip factor. Fig. 3.4 demonstrate that the rate of fluid transport at the starting point shows no variation but soon starts decreasing for a while and then accelerated. With distance and rise in slip factor, the sufficient fluid slip through the plate and thus it increases the fluid velocity finally. The fluid velocity rises with the growth of β as noticed from Fig.3.5. The reason behind this is the effect of buoyancy force which arises because of the positive mixed convection parameter in presence of slip factor.

The impacts of k_1, λ, Pr, β on the fluid temperature profile are demonstrated from Fig. 3.6, 3.7, 3.9, and 3.10. It is observed that with the growth of k_1, λ, Pr, and β, the fluid temperature diminish. As fluid becomes more viscous with increasing k_1 it hinders the transition of thermal energy to the fluid easily and thus temperature curves decrease. The

growth of λ lowered the thermal diffusivity of the fluid which reduces the energy capability and the thickness of thermal boundary layer. The relative thickness of the thermal boundary layer controlled by Pr and its growth reduces the thermal diffusivity and thus temperature reduces. The fluid temperature reduces with rising values of thermal slip parameter β as less amount of heat is deported from the plate to the fluid. The fluid temperature gradually lowered with increasing distance from the origin and thus there is a transition of thermal energy from the fluid towards the plate. Fig.3.8 shows that the temperature of the fluid accelerates with the growth of the velocity slip factor. As more fluid passes through the plate with an increasing velocity slip factor, it enhances the fluid temperature.

The effects of flow feature factors k_1, λ,δ, Pr, and β on the magnitude of the rate of temperature are explained from Fig. 3.11 to 3.15. The direction and the rate at which temperature changes about the certain locations of the fluid termed as temperature gradient. Figures 3.11, 3.12, and 3.14 signifies that the rate of change of temperature gets lowered initially with the growth of k_1, λ, Pr but gradually enhances for rising values of stated parameters and distance. The deviation of the rate of change of temperature is observed due to dominant viscosity factor and buoyance effects. But from Fig. 3.13 reverse behavior of the temperature gradient is noticed for increasing velocity parameter. Fig. 3.15 shows that the growth of the thermal slip parameter changes the rate of direction of the temperature from the plate to the fluid.

The graphical representation of the rate of change of temperature on the plate for variation of $k_1$against δ and β are plotted in Fig.16 andFig. 3.17. Fig. 3.16 indicates that the changing rate of temperature at the plate increases with the growth of k_1 and δ. The rising values of visco-elasticity and velocity slip factors help to enhance the amount of thermal transition of heat from the fluid to the vertical plate. Fig.3.17 indicates that the temperature gradient at the plate rises with the growth of k_1 but diminishes with increasing values of β. The heat transfer can be controlled by adjusting the thermal slip factor.

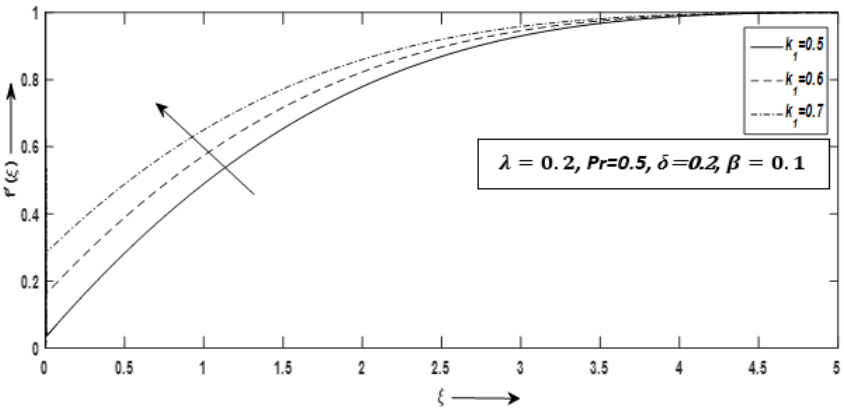

Fig. 3.2: Velocity curves $f'(\xi)$ against ξ for k_1

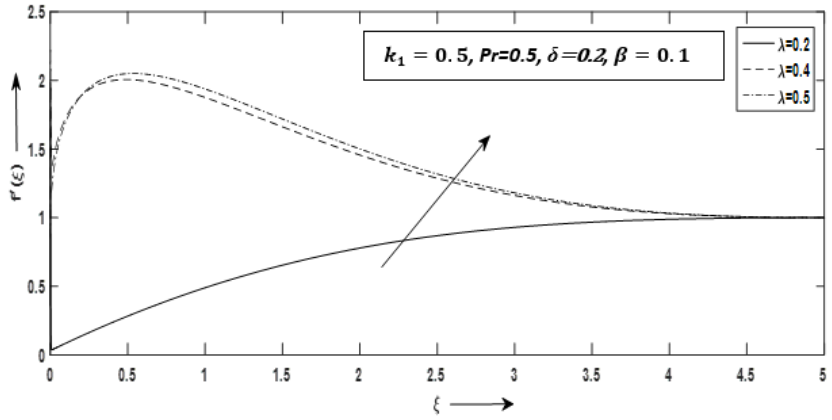

Fig. 3.3: Velocity curves $f'(\xi)$ against ξ for λ

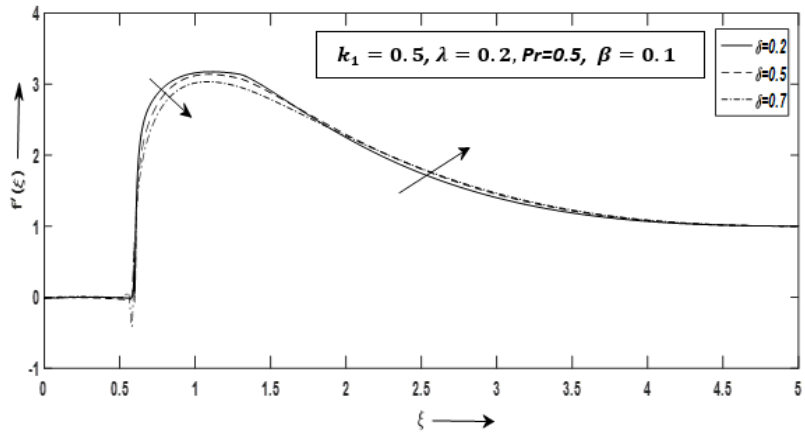

Fig. 3.4: Velocity curves $f'(\xi)$ against ξ for δ

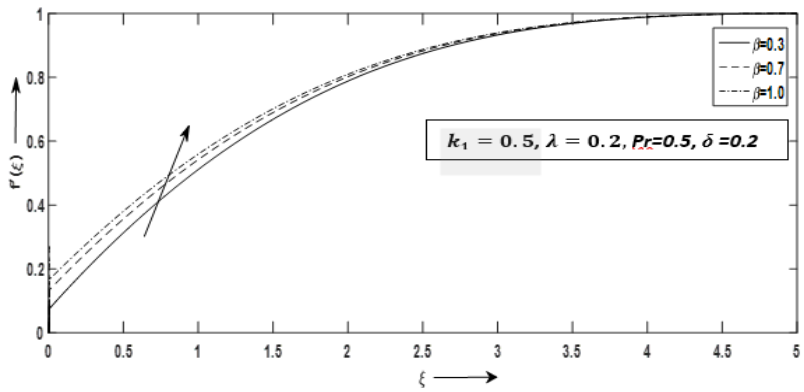

Fig. 3.5 Velocity curves $f'(\xi)$ against ξ for β

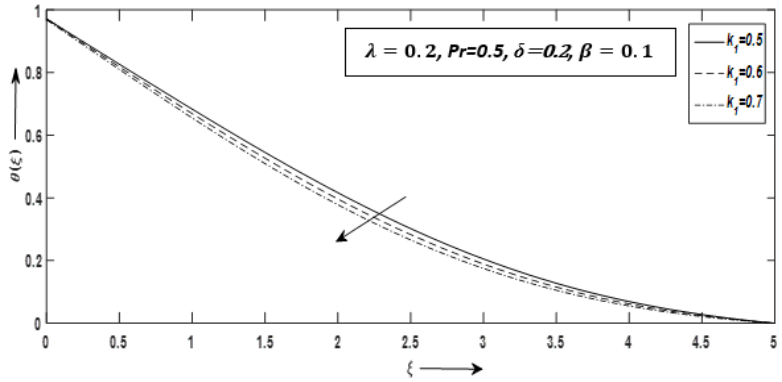

Fig. 3.6 Temperature curves $\theta(\xi)$ against ξ for k_1

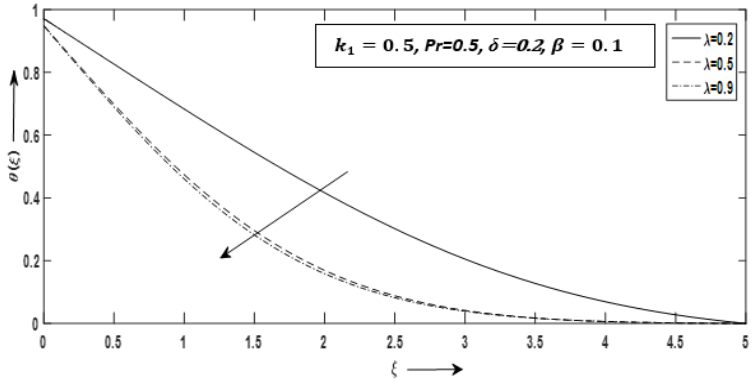

Fig. 3.7 Temperature curves $\theta(\xi)$ against ξ for λ

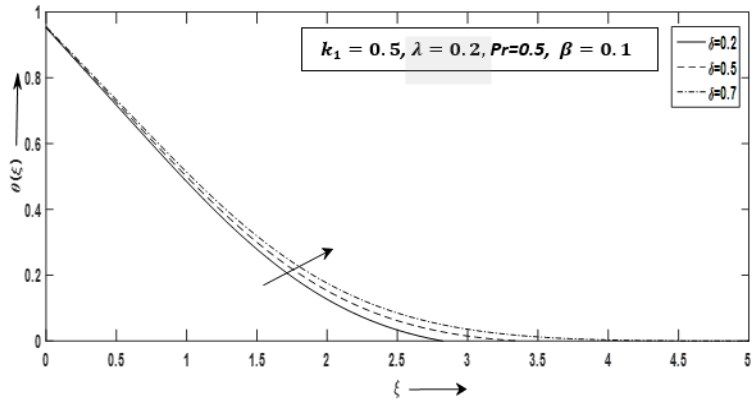

Fig. 3.8 Temperature curves $\theta(\xi)$ against ξ for δ

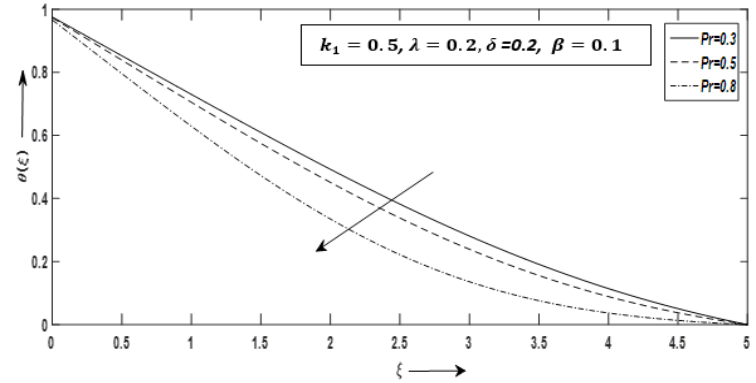

Fig. 3.9: Temperature curves $\theta(\xi)$ against ξ for Pr

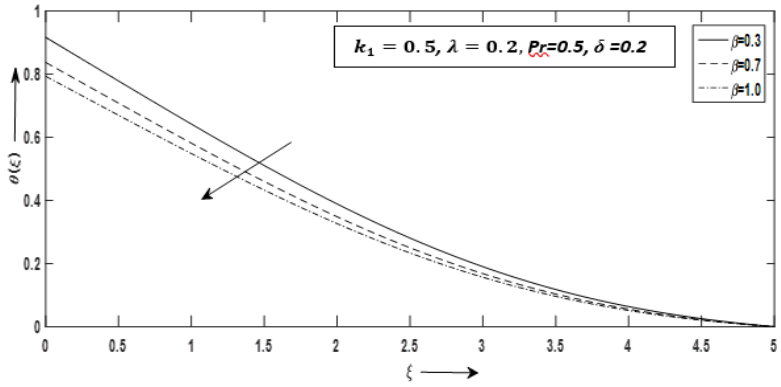

Fig. 3.10 Temperature curves $\theta(\xi)$ against ξ for β

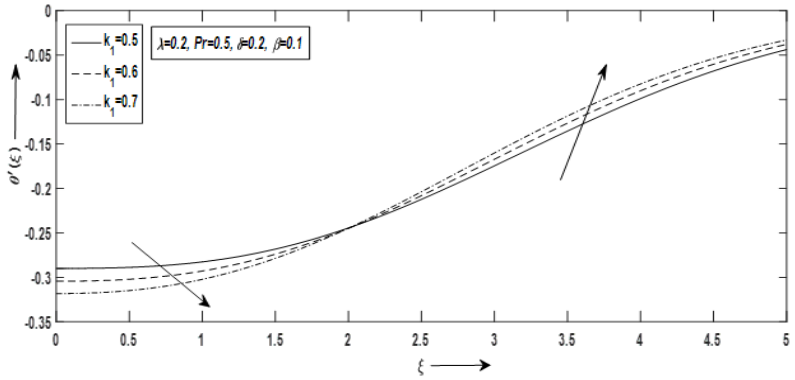

Fig. 3.11: Temperature gradient curves $\theta'(\xi)$ against ξ for k_1

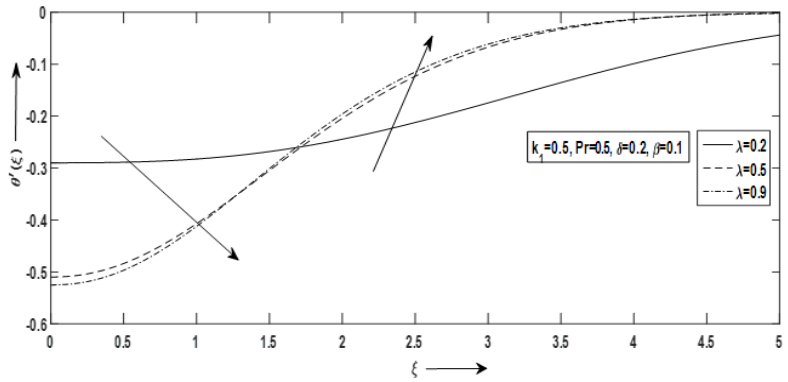

Fig. 3.12: Temperature gradient curves $\theta'(\xi)$ against ξ for λ

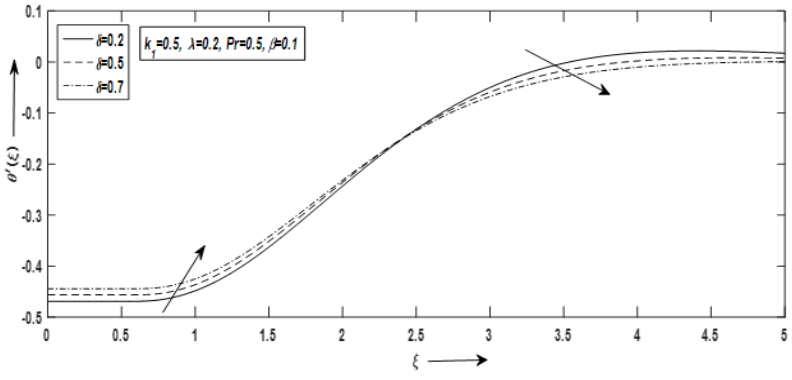

Fig. 3.13: Temperature gradient curves $\theta'(\xi)$ against ξ for δ

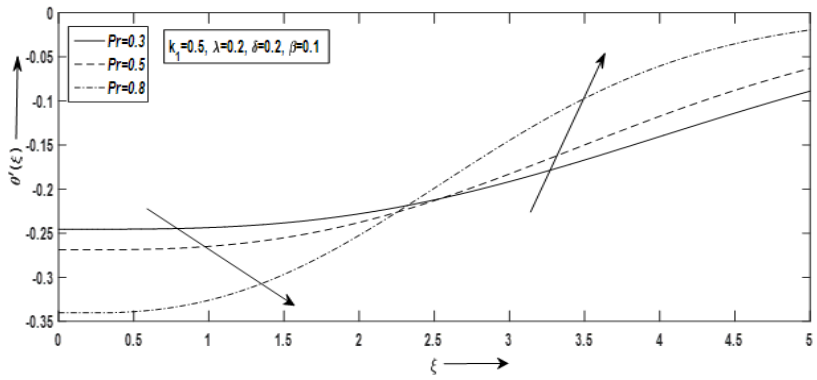

Fig. 3.14: Temperature gradient curves $\theta'(\xi)$ against ξ for Pr

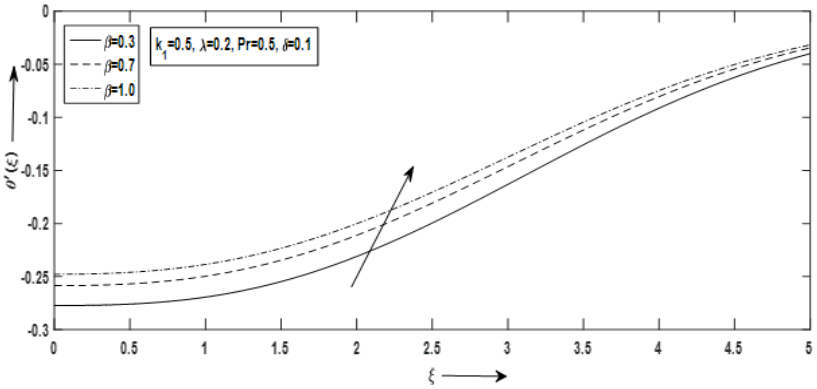

Fig. 3.15: Temperature gradient curves $\theta'(\xi)$ against ξ for β

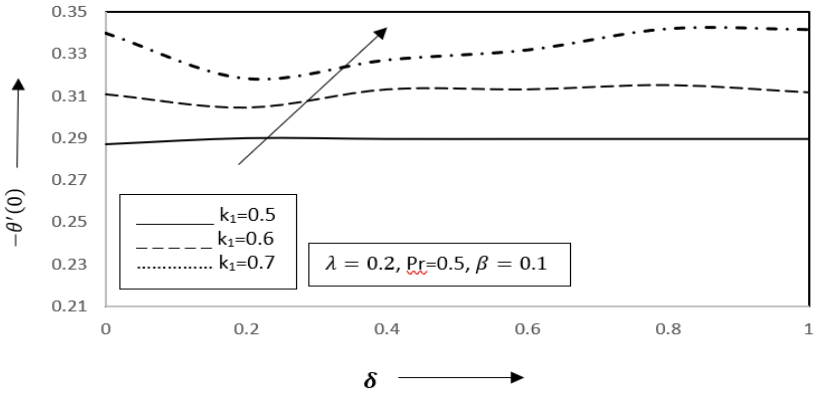

Fig. 3.16: Variation of $-\theta'(0)$ against δ for k_1

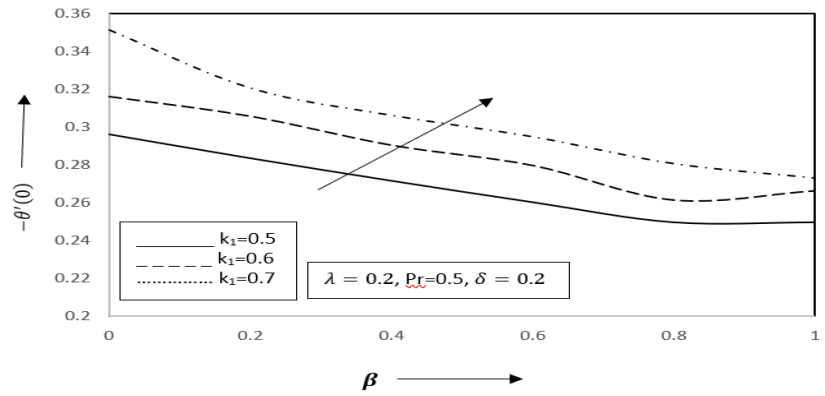

Fig. 3.17: Variation of $-\theta'(0)$ against β for k_1

3.5 Conclusions

The motion of steady mixed convective visco-elastic incompressible boundary layer fluid over a vertical plate along with slip factor at the boundary has been analyzed. The impact of dominant flow feature factors over velocity, temperature, and temperature gradient are studied. The numerical computation is performed with finite difference method based 'bvp4c' solver and results are plotted for visualization and discussions. The fluid domain is highly influenced by the elastic-viscous, mixed convection, and slip parameters. The results reveal various aspects of the additional terms in the constitutive equations for the non-Newtonian visco-elastic fluid model as compared to the Newtonian fluid model. There is a lot of future scopes to extend this work. The unsteady case may be considered to study fluid motion under the same geometrical conditions. The different analytical and numerical methods can also be applied to compare the obtained results. The simulation of the numerically computed results may give a clear picture of the fluid flow.